Department of
Industry and Resources

RECORD
2006/10

INTERPRETED BEDROCK GEOLOGY OF THE NORTHERN MURCHISON DOMAIN YOUANMI TERRANE, YILGARN CRATON

by C. V. Spaggiari

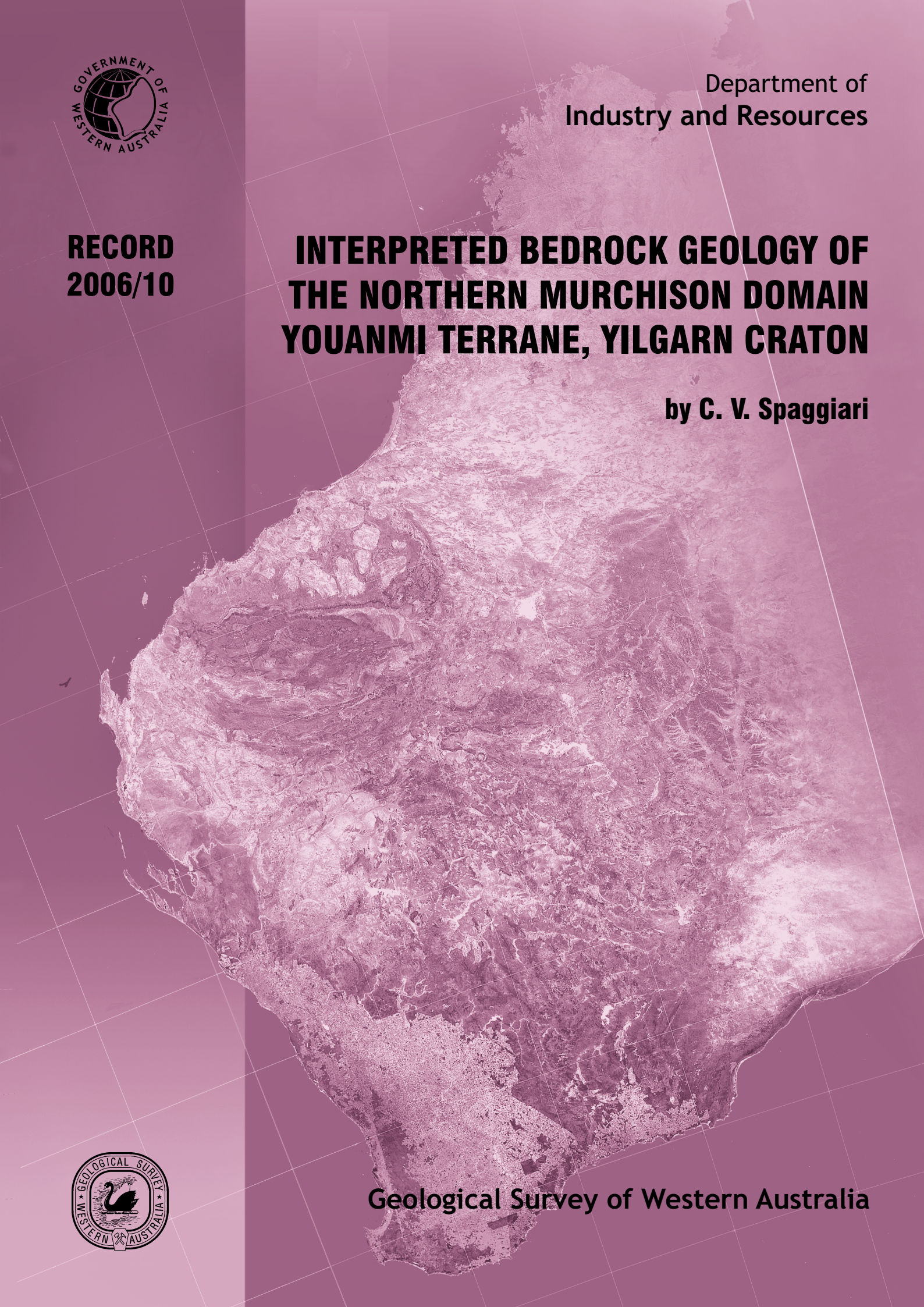

Geological Survey of Western Australia

MINISTER FOR RESOURCES
Hon. John Bowler MLA

DIRECTOR GENERAL, DEPARTMENT OF INDUSTRY AND RESOURCES
Jim Limerick

EXECUTIVE DIRECTOR, GEOLOGICAL SURVEY OF WESTERN AUSTRALIA
Tim Griffin

ERRATA
Figures 1, 2, and 11 have been modified.
As at June 2005

REFERENCE
The recommended reference for this publication is:
SPAGGIARI, C. V., 2006, Interpreted bedrock geology of the northern Murchison Domain, Youanmi Terrane, Yilgarn Craton: Western Australia Geological Survey, Record 2006/10, 19p.

National Library of Australia Card Number and ISBN 1 74168 045 X

Grid references in this publication refer to the Geocentric Datum of Australia 1994 (GDA94). Locations mentioned in the text are referenced using Map Grid Australia (MGA) coordinates, Zone 50. All locations are quoted to at least the nearest 100 m.

Cover image modified from Landsat data, courtesy of ACRES

Published 2006 by Geological Survey of Western Australia
This Record is published in digital format (PDF) and is available online at www.doir.wa.gov.au/gswa/onlinepublications.
Laser-printed copies can be ordered from the Information Centre for the cost of printing and binding.

Further details of geological publications and maps produced by the Geological Survey of Western Australia are available from:
Information Centre
Department of Industry and Resources
100 Plain Street
EAST PERTH, WESTERN AUSTRALIA 6004
Telephone: +61 8 9222 3459 Facsimile: +61 8 9222 3444
www.doir.wa.gov.au/gswa/onlinepublications

GEOLOGICAL SURVEY OF WESTERN AUSTRALIA

Record 2006/10

INTERPRETED BEDROCK GEOLOGY OF THE NORTHERN MURCHISON DOMAIN, YOUANMI TERRANE, YILGARN CRATON

by
C. V. Spaggiari

Perth 2006

Contents

Figures

Interpreted bedrock geology of the northern Murchison Domain, Youanmi Terrane, Yilgarn Craton

by

C. V. Spaggiari

Abstract

Newly acquired aeromagnetic data, remote-sensing data, pre-existing maps, and some new fieldwork have provided the basis for an interpreted bedrock geology and structural map of the northern part of the Murchison Domain of the Youanmi Terrane, Yilgarn Craton. The map was created in a GIS program to provide the best spatial accuracy possible, and to use the datasets as layers to maximize the amount of information at particular points as an aid to interpretation. The map includes new structural interpretations, and adds to the understanding of the geology under cover.

The most widely published structural model of the region was largely based on localized fold superposition, and extrapolated across the entire domain. Although detailed mapping is required to test this model, the aeromagnetic data do not fully support it, particularly in the Meekatharra–Wydgee greenstone belt and surrounds. The structure of the Murchison Domain is complex and potentially heterogeneous across different parts of the domain. Granitic intrusions have substantially modified the geometry of the greenstone successions and their structure, and this must be taken into account when interpreting large-scale fold patterns and structural chronology. In the interpreted bedrock geology map presented here no attempt has been made to fit the lithological units into a stratigraphic scheme. The limited available geochronological data have shown that the stratigraphy for the Murchison Domain is problematic and further work is required to establish primary relationships, especially within the greenstones.

An approximately 50 to 60 km-wide, northeast-trending, shear-dominated structural zone incorporating the Meekatharra area, and extending through the Cue area at least as far south as Mount Magnet (i.e. taking in a large part of the Meekatharra–Wydgee greenstone belt), has been interpreted primarily from the aeromagnetic images. A major structure identified in this zone is the northeast-trending Chunderloo Shear Zone, which has a dextral sigmoidal pattern in the aeromagnetic images, and is dominated by dextral kinematic indicators in the field. Near Mount Magnet, the structural zone changes to a northerly trend where faults and shears cut through granitic rocks, as well as the Windimurra and Narndee layered intrusions. The western side of the northeast-trending part of the structural zone is marked by a west-dipping thrust that separates two distinctive regions of different structural style, with the western side less shear dominated and preserving more evidence of an earlier structural history. Large, approximately easterly trending shears and faults cut across the Jack Hills greenstone belt in the northwest and appear to extend sufficiently south to at least truncate the northern part of the Mingah Range greenstone belt. These structures are Paleoproterozoic in age and related to the Capricorn Orogeny.

KEYWORDS: Murchison Domain, Youanmi Terrane, Yilgarn Craton, aeromagnetic interpretation, regional deformation.

Introduction

The Yilgarn Craton of Western Australia is divided into four tectonic units: the Narryer Terrane, the Eastern Goldfields Superterrane, the Youanmi Terrane, and the South West Terrane (Fig. 1; Cassidy et al., 2006). The Youanmi Terrane is an amalgamation of the former Southern Cross and Murchison Terranes. Recent mapping in the central Yilgarn Craton and the results of a geochemical and geochronological study of granitic rocks of the Yilgarn Craton (Cassidy et al., 2002; Geological Survey of Western Australia, in prep.a) have shown that there is no basis for the long-standing division into two separate terranes, and the Murchison Domain and Southern Cross Domain are recognized within the Youanmi Terrane.

The interpreted bedrock geology map presented in this Record covers the northern part of the Murchison Domain and a small part of the southeastern part of the Narryer

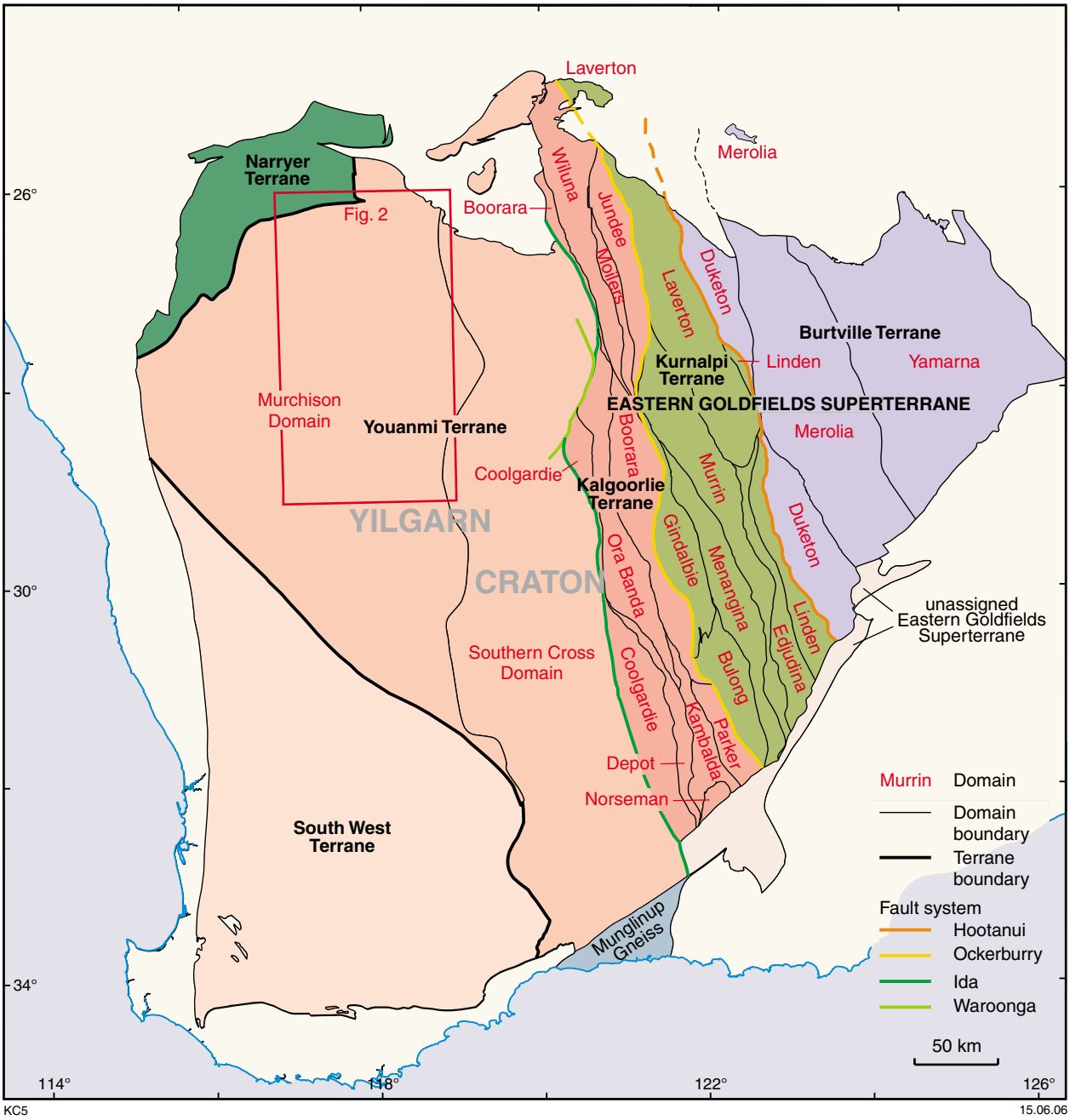

Figure 1. **Map of the Yilgarn Craton (after Cassidy et al., 2006) showing the Youanmi Terrane, which is an amalgamation of the former Southern Cross and Murchison Terranes. The location of the interpreted bedrock geology map of the northern Murchison Domain (Fig. 2) is also shown**

Terrane. It extends from the Jack Hills greenstone belt in the northwest to the Youanmi Shear Zone in the southeast (Figs 1 and 2) and covers the (1:250 000) map sheets of BELELE*, CUE, KIRKALOCKA, the northern part of NINGHAN, the western thirds of GLENGARRY, SANDSTONE, and YOUANMI, and the northwest of BARLEE. The geology is dominated by greenschist- to lower amphibolite-facies Archean granites and greenstones, and includes large layered intrusions in the southern part.

* Capitalized names refer to standard 1:250 000 map sheets.

Purpose and scope

This Record provides background information to the interpreted bedrock geology and structural map presented in the Murchison geological exploration package (Geological Survey of Western Australia, 2006). It is not intended as a detailed account of the geology of the Murchison Domain, but provides a summary and references to more detailed work, and points out outstanding issues regarding the present understanding of the geology. The methodology used to create the interpreted bedrock geology and structural map is

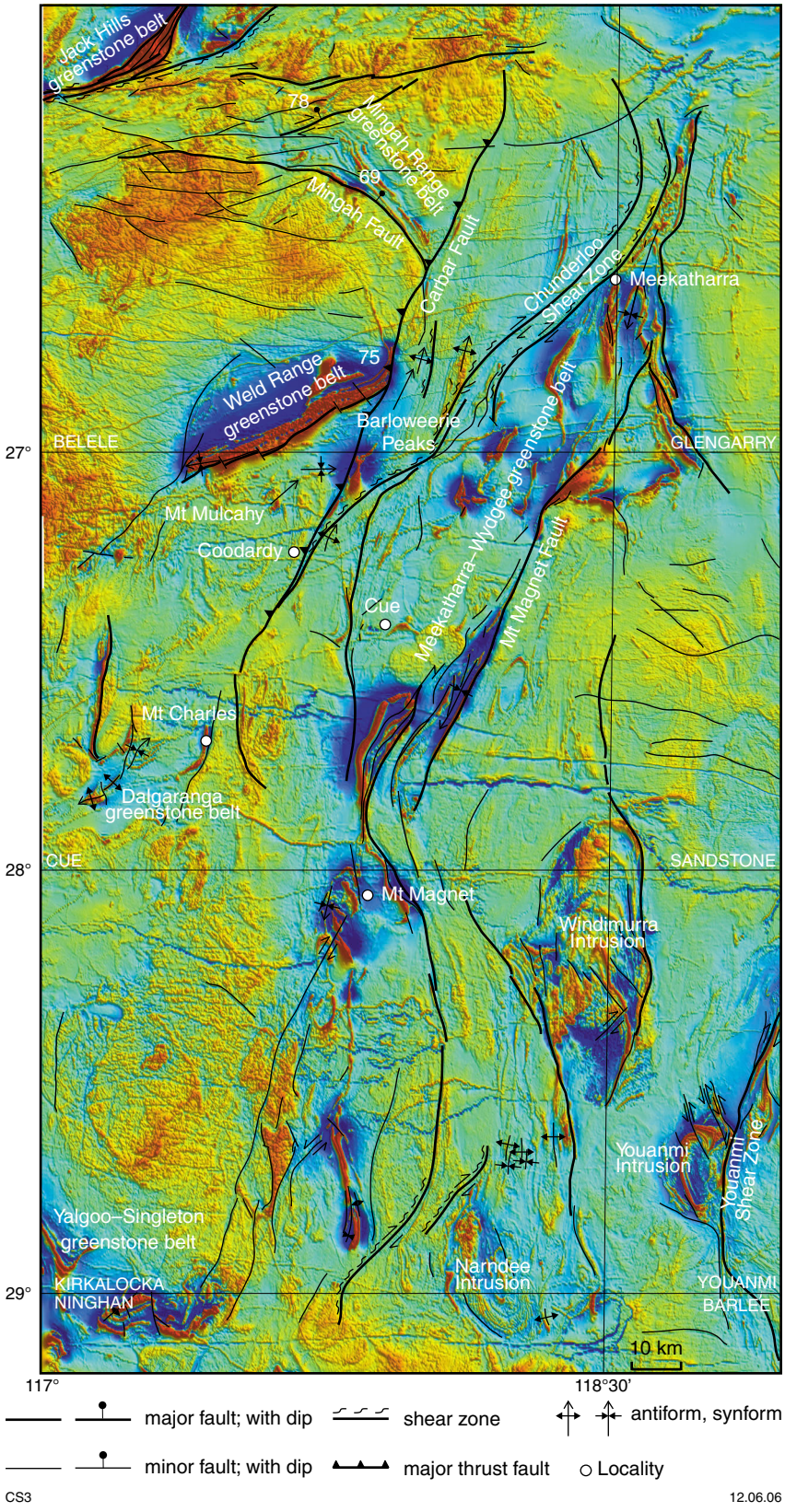

Figure 2. Simplified interpreted structural map of the northern Murchison Domain, showing localities and major structures, overlain on a reduced to pole, total magnetic intensity image. Structures shown are derived from the interpreted bedrock geology map in Geological Survey of Western Australia (2006), Hallberg (2000), GSWA's 1:250 000-scale geological series map sheets, and Watkins and Hickman's (1990a) 1:500 000 geological map

outlined, and its limitations addressed. Although the map can be viewed at any scale, it was compiled at a nominal 1:100 000 scale, suitable for display or printing at either 1:250 000 or 1:500 000 scale.

Previous work and structural models

The Murchison Domain occupies a large part of the Yilgarn Craton, but there have been few published studies of the region. Two models of granite–greenstone formation have been proposed to explain what has been perceived as a domical pattern of granites surrounded by arcuate belts of greenstones. Gee (1979) proposed formation by diapirism where relatively buoyant granites intrude a more dense greenstone cover creating gravitational instability that causes the greenstones to sink into the granites and form large synclinal 'keels'. Myers and Watkins (1985) and Watkins and Hickman (1990a) suggested that the domical patterns were antiformal domes produced by superimposed folding episodes at high angles that post-dated magmatism. The superimposed folding pattern interpretation has been challenged by Rey et al. (1999) who interpreted the domes as the result of deformation during magmatism, most likely in a transpressional regime. Crucial to any of these models is an understanding of the 3D geometry, structural chronology, and timing of deformation relative to magmatism. It should be noted that the interpretation of Myers and Watkins (1985) was derived primarily from mapping in the Yalgoo area, just west of the area covered by the present study area; however, their interpretation was applied to the whole of the Murchison Domain.

A structural chronology was proposed by Watkins and Hickman (1990a) comprising four regional phases of deformation. D_1 was interpreted to have produced subhorizontal structures such as recumbent folds and to be confined to some pegmatite-banded gneiss and the interpreted lower succession of the greenstones (Luke Creek Group, Figs 3 and 4). D_2 and D_3 were assumed to have affected the whole of the Murchison Domain, producing tight to isoclinal, upright folds at high angles resulting in the interpreted fold-superposition pattern. In this scheme, D_3 occurred under higher strain conditions and produced the dominant, north- to northeast- and north- to northwest-trending regional foliation. D_4 deformation was interpreted to have been part of the same east–west compression event as D_3, and produced extensive shears and faults. While this scheme may be correct in part it is not clear whether it can be extrapolated across the whole domain as it assumes that the stratigraphy is correct and that, apart from the D_1 event and some possible 'post-folding' granites, the deformation affected all rocks of the Murchison Domain, that is, they were all formed after D_1 and before D_2. It also assumes that the deformation was uniform in intensity and style across the whole domain. These issues exist because there is poor geochronological control, and because it was assumed that local structural chronology could be extrapolated across the whole region. Where extensive shearing has occurred, such as in the central area encompassing the Meekatharra–Wydgee greenstone belt, this could be problematic because these areas are complex and it is possible that localized shear-related folding could be misinterpreted as part of a separate event.

Lithologies, stratigraphy, and geochronology

The northern Murchison Domain is made up almost entirely of Archean granitic rocks, greenstones, and mafic–ultramafic intrusions. Within the study area outliers of Paleoproterozoic sedimentary rocks outcrop in the north (Yerrida Basin; Piranjo et al., 2004), and abundant mafic dykes of predominantly Mesoproterozoic age crosscut major structures (Wingate et al., 2004). Limited geochronological studies undertaken in the Murchison Domain show that most greenstones and granitic rocks were deposited or emplaced between c. 3000 and 2600 Ma (e.g. Pidgeon and Hallberg, 2000).

Greenstones

The greenstones of the Murchison Domain include metamorphosed mafic, ultramafic, sedimentary, and volcanic sequences that vary in abundance and character from belt to belt, but are dominated by mafic rocks. Watkins and Hickman (1990a) defined a stratigraphic scheme made up of two groups, the basal Luke Creek Group and the overlying Mount Farmer Group, which together formed the Murchison Supergroup (Fig. 4). The Luke Creek Group consisted of four formations comprising two volcanic sequences: one dominated by tholeiitic and komatiitic basalt, banded iron-formation (BIF) and interlayered mafic rocks, and the second by an ultramafic intrusive–volcanic complex, interlayered tholeiitic and komatiitic basalt, mafic and felsic volcanic rocks and associated sedimentary rocks, and jaspilitic BIF. The Mount Farmer Group was interpreted as a series of formations with limited lateral extent that differ in character between greenstone belts. It consisted of metamorphosed tholeiitic and komatiitic basalt, ultramafic rocks, gabbroic and doleritic sills, felsic volcanic rocks and associated sedimentary rocks, BIF, and minor pelitic and psammitic schists, metashale, metasandstone and metaconglomerate. The stratigraphic scheme of Watkins and Hickman (1990a) has been questioned by Pidgeon and Hallberg (2000) who divided the greenstone sequences of the northern Murchison Domain into five informal assemblages consisting of ultramafic, mafic, and felsic volcanic rocks including komatiite, komatiitic basalt, andesite, BIF, black shale, chert, and volcanic sandstone (Assemblages 1–3); felsic volcanic rocks of mostly rhyolitic to dacitic composition and associated sedimentary rocks (Assemblage 4); and graphitic clastic rocks and various sedimentary rocks spatially related to major faults (Assemblage 5; Fig. 5). They argued that it was difficult to correlate units across greenstone belts because of structural complexity and separation by granitic intrusions. Their assemblages are defined in terms of rock associations and are not necessarily time equivalents. They proposed that assemblages 1 to 3 were deposited without major breaks and were overlain by the spatially limited

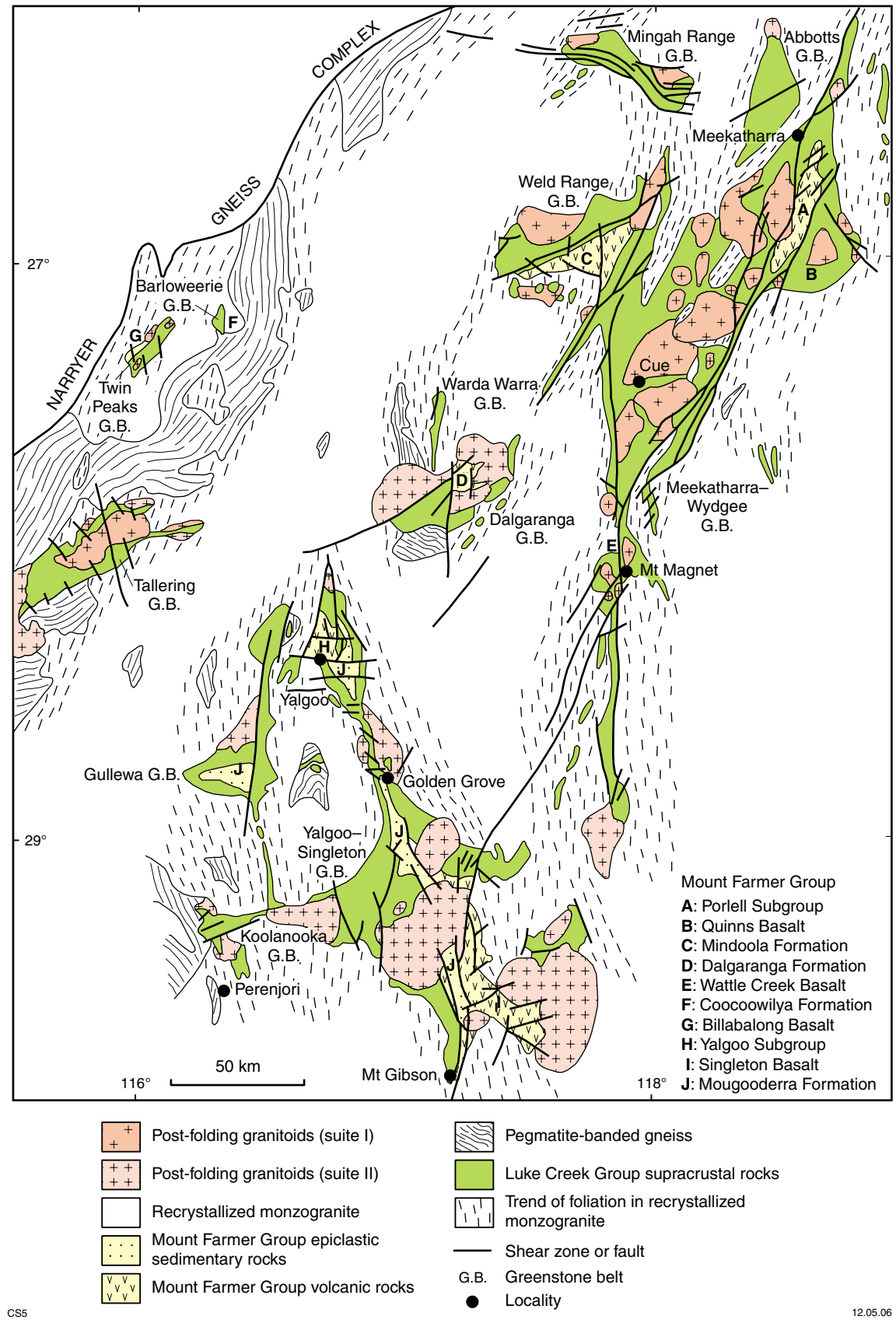

Figure 3. Simplified geology of the Murchison Domain of Watkins and Hickman (1990b), showing greenstone belts and major structures and stratigraphy

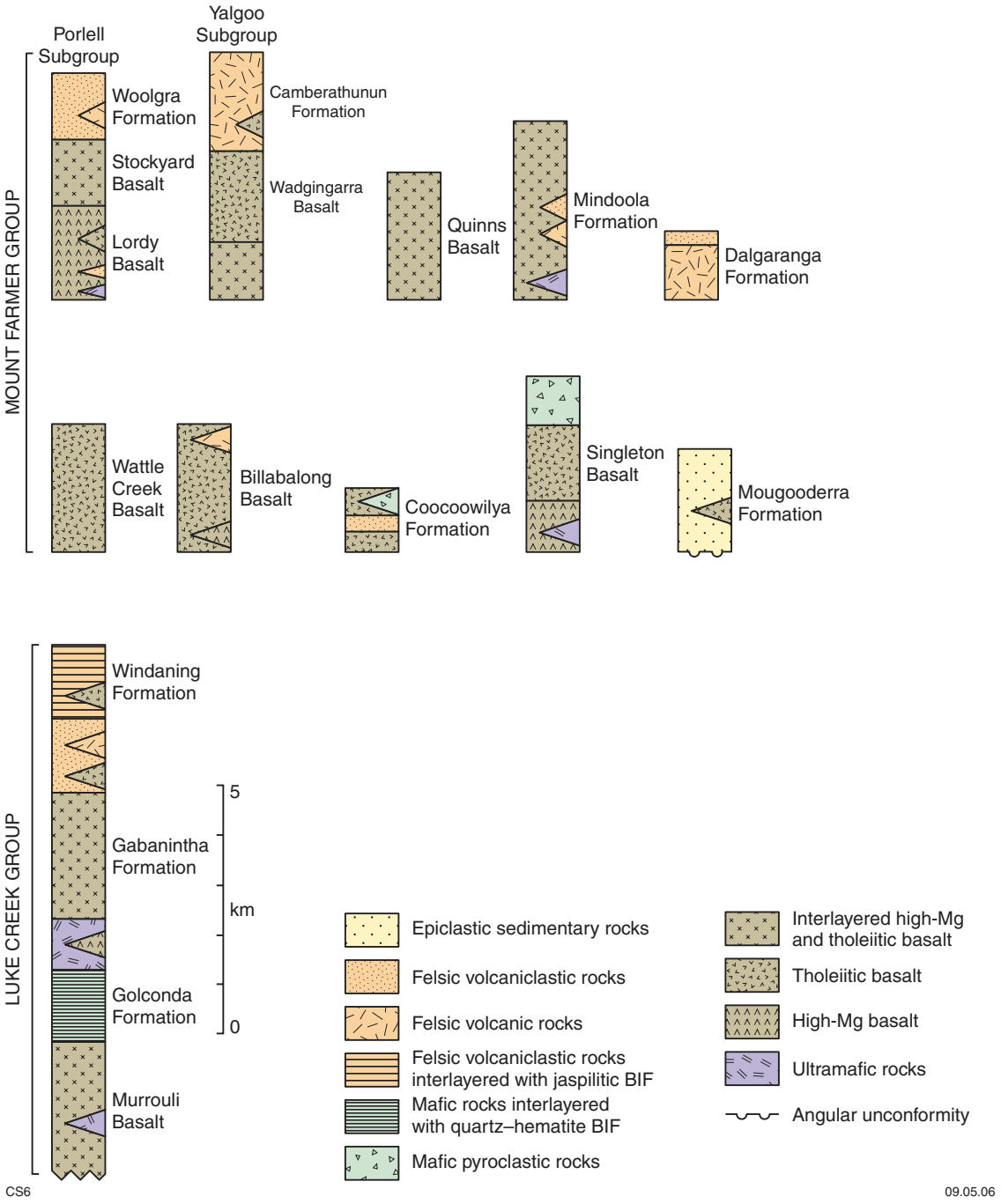

Figure 4. Murchison Supergroup stratigraphy of Watkins and Hickman (1990b), showing groups, subgroups, formations, and rock types. Stratigraphic thicknesses are approximate and variable along strike

assemblages 4 and 5. These assemblages are described in detail in Hallberg (2000).

The available geochronological data indicate that the majority of felsic volcanic rocks formed between c. 2750 and 2700 Ma, but some older volcanic rocks are present at least locally. Whether these ages also represent typical ages of the mafic components of the greenstone belts is unknown because mafic rocks are difficult to date directly, and field relationships with the felsic rocks are uncertain. Pidgeon and Wilde (1990) dated zircons from felsic volcaniclastic rocks at Golden Grove in the western part of the Murchison Domain (Fig. 3) using conventional single grain U–Pb methods. Their results indicated that felsic volcanic activity occurred between c. 2957 and 2951 Ma (revised ages of Pidgeon et al., 1994; reported in Wang et al., 1998). These ages are in agreement with those of Wang et al. (1998) who reported sensitive high-resolution ion microprobe (SHRIMP) U–Pb zircon ages from rhyolitic to dacitic rocks from the Luke Creek Group (Gabanintha Formation), also at Golden Grove, ranging from 2960 ± 6 to 2945 ± 4 Ma.

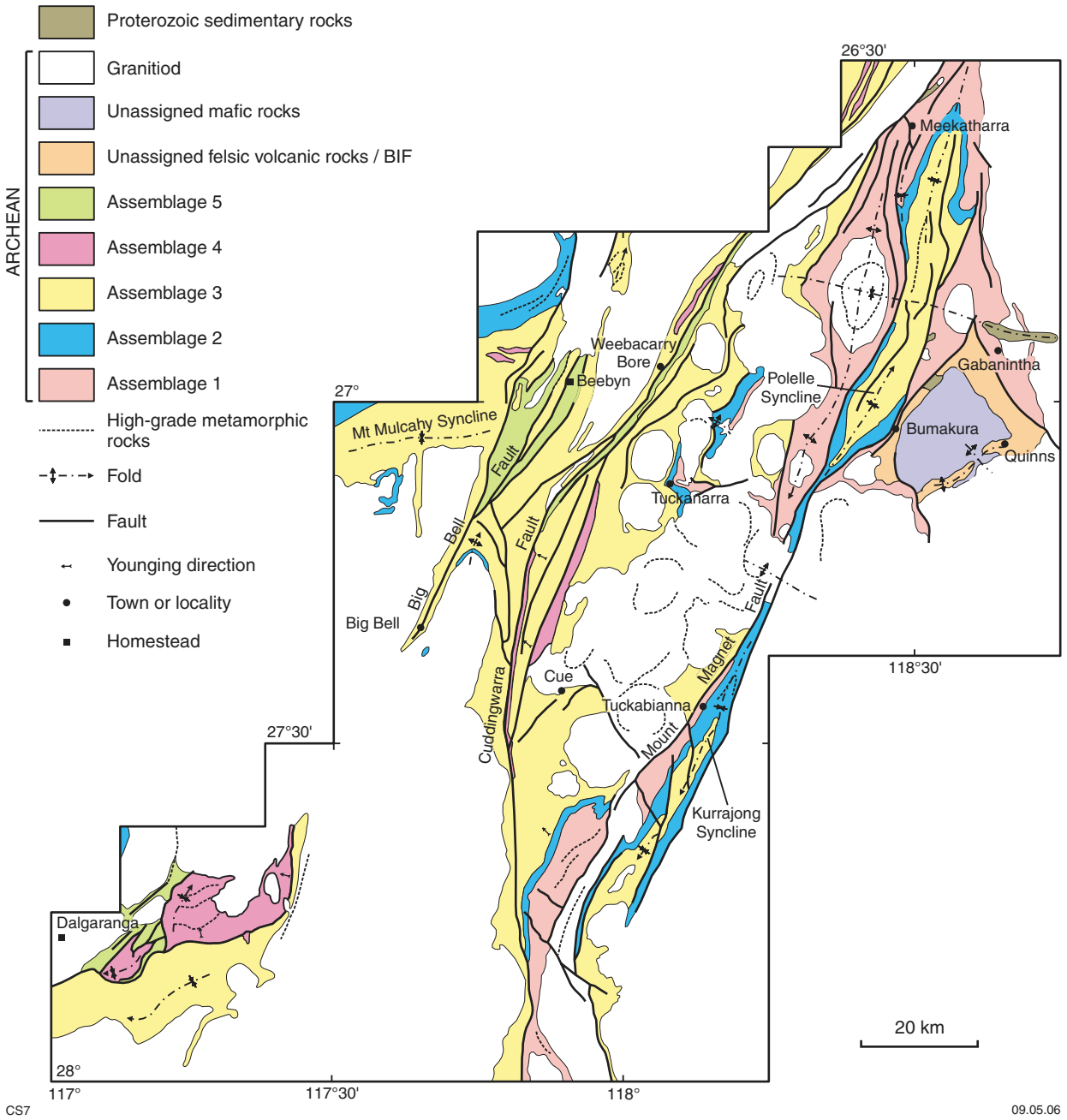

Figure 5. Simplified geological map of the northern Murchison Domain showing mapped and interpreted structures and the lithological assemblages of Pidgeon and Hallberg (2000)

They also dated zircons from a reworked volcanogenic sandstone from the overlying Windaning Formation and found that it was deposited about 140 million years later. This highlighted problems with the stratigraphy of Watkins and Hickman (1990a), showing that the Windaning Formation could not be part of the Luke Creek Group. Schiøtte and Campbell (1996) also suggested that the Windaning Formation was too young to be part of the Luke Creek Group based on U–Pb zircon ages they obtained from cherts in the Mount Magnet area that were no older than 2800 Ma. Pidgeon and Hallberg (2000) showed that felsic volcanism (their Assemblage 4) varied in age from locality to locality, with both SHRIMP U–Pb zircon and conventional single-grain U–Pb zircon ages of 2749 ± 4 to 2743 ± 4 Ma in the Dalgaranga greenstone belt, and ages of 2762 ± 4, 2761 ± 1, 2716 ± 4, and 2750 to 2700 Ma from several localities near Cue.

Yeats et al. (1996) dated zircons from felsic schist (interpreted as subvolcanic rocks) from the Mount Gibson mine (Windaning Formation, Luke Creek Group, southern Yalgoo–Singleton greenstone belt, Fig. 3) using SHRIMP U–Pb zircon geochronology and found two populations at 2934 ± 6 and 2627 ± 13 Ma. They interpreted the older group as a crystallization

age of the igneous precursor to the schist and the younger group as hydrothermal zircons related to alteration and gold mineralization, as well as granite emplacement. The date for the older group is within error of a zircon population from another schist (quartz porphyry) they dated at 2929 ± 3 Ma and interpreted as a minimum crystallization age. This rock also has a variety of zircon ages, with some as young as 2730 ± 3 Ma. These schists have complex zircon U–Pb systematics that are difficult to interpret and it is possible that the older grains are inherited (see also Pidgeon and Hallberg, 2000). Schiøtte and Campbell (1996) dated zircons using SHRIMP U–Pb from felsic volcanic rocks from the Mount Farmer Group in the Mount Magnet area that ranged in age from 2739 ± 11 to 2702 ± 10 Ma, suggesting that the Mount Farmer Group, at least in that area, was deposited as late as c. 2700 Ma.

Layered mafic–ultramafic intrusions

In the southern part of the interpreted map area (mostly on KIRKALOCKA and YOUANMI, Fig. 2) are three large mafic–ultramafic intrusions — the Windimurra, Narndee, and Youanmi Intrusions — that may have been emplaced synchronously, and subsequently separated by shear zones and granitic intrusions. The Windimurra Intrusion is the largest of these and covers an area of about 2345 km^2, but only about 10% is exposed (Ahmat and Ruddock, 1990). It is dominated by coarse-grained, plagioclase-rich layered cumulates of several types of gabbroic rocks, and minor amounts of serpentinized dunite, chromitite, and magnetitite (Mathison et al., 1991). The intrusion is surrounded by monzogranites with sheared or strongly deformed contacts, and is in part overlain by felsic volcanic rocks, volcanic sandstone, BIF, chert, granophyre and dolerite (Kantie Murdana Volcanics) that may be remnants of roof pendants or younger cover rocks (Mathison et al., 1991). Zircons from a rhyolite from the Kantie Murdana Volcanics have a SHRIMP U–Pb age of 2813 ± 3 Ma (Nelson, 2000). The Windimurra Intrusion also includes magnetite-bearing cumulates that contain vanadium, and some occurrences of cumulates rich in platinum group elements (Mathison et al., 1991). Unpublished Sm–Nd whole-rock and mineral data suggest that the intrusion evolved at about 2800 Ma (reported in Ahmat and Ruddock, 1990).

The Narndee Intrusion is also dominated by cumulate gabbroic rocks, but the northern part has a higher proportion of ultramafic rocks (peridotite, dunite, and olivine pyroxenite) than the southern part and the Windimurra Intrusion (Ahmat and Ruddock, 1990). This has been interpreted to reflect exposure of deeper levels of the intrusion in the north (Ahmat and Ruddock, 1990). The Narndee Intrusion has been interpreted as a north-plunging synclinal structure with a core of metasedimentary rocks, BIF, and felsic volcanic rocks, possibly in tectonic contact with the underlying intrusive rocks (Ahmat and Ruddock, 1990).

Granitic rocks

Granitic rocks in the Murchison Domain are dominated by monzogranites, including porphyritic, banded, and even-grained varieties, showing variable degrees of recrystallization and foliation development. Watkins and Hickman (1990a) divided the granites into four suites, emplaced in the following order: pegmatite-banded gneiss, recrystallized monzogranite, and two suites of 'post-folding' granitic rocks (Fig. 3). Rafts and xenoliths of greenstones (e.g. BIF and amphibolite), some up to several kilometres in length, are abundant locally (Watkins et al., 1987; Watkins and Hickman, 1990a). The two suites of 'post-folding' granitic rocks were divided according to petrology and geochemistry with suite I comprising tonalite, granodiorite, monzogranite, and trondhjemite, and suite II comprising quartz-rich monzogranite and syenogranite. These plutons are commonly small and characterized by subcircular or elliptic patterns that are distinctive on the aeromagnetic images. Although they have been termed 'post-folding', they commonly show sheared or deformed margins (e.g. Watkins and Hickman, 1990a) that could be related to folding as well as shearing. Dating of zircons from 'post-folding' or 'post-tectonic' granites and deformed granites has shown that, in some instances, the undeformed granites are older than the deformed granites (Schiøtte and Campbell, 1996, see below). This indicates that the effects of deformation are heterogeneous due to rheology contrasts and strain partitioning, and that the granites cannot be divided on the basis of foliation or fold development.

Cassidy et al. (2002) divided the granitic rocks of the Yilgarn Craton on the basis of petrology and geochemistry. In the northern Murchison Domain the bulk of the granitic rocks are high-Ca and low-Ca varieties, with less extensive high-HFSE (high field strength element) and mafic granites commonly associated with greenstones (Champion and Cassidy, 2002). A major geochemical change appears to have occurred across the Yilgarn Craton at c. 2655 Ma, shown by the change from dominantly high-Ca to dominantly low-Ca granitic magmatism (Cassidy et al., 2002), but in the northern Murchison Domain high-Ca magmatism appears to have mostly ended by c. 2670 Ma (Champion and Cassidy, 2002). Most of the granitic rocks of the Murchison Domain appear to have formed between c. 2750 and 2610 Ma, apart from some recrystallized monzogranite near Mount Gibson, interpreted to have a magmatic SHRIMP U–Pb zircon age of 2935 ± 3 Ma (Yeats et al., 1996), and pegmatite-banded gneiss from near Yalgoo dated at c. 2919 ± 12 Ma (Weidenbeck and Watkins, 1993). Most grains from both of these samples are strongly discordant with only a few grains concordant at around the interpreted ages. These data are difficult to interpret and it is possible that these older grains are inherited. More robust are SHRIMP zircon ages (Schiøtte and Campbell, 1996; Mueller et al., 1996) of 2716 to 2696 Ma for granite plutons from within greenstone belts, previously described as undeformed (Watkins and Hickman, 1990a), 2710 to 2640 Ma for recrystallized monzogranites, and 2700 ± 7 Ma for a granodiorite near Cue. SHRIMP U–Pb zircon ages from recrystallized monzogranites dated by Wiedenbeck and

Watkins (1993) fall between 2704 ± 51 and 2681 ± 6 Ma, and for their 'post-folding' granites between 2641 ± 5 and 2602 ± 14 Ma. Mueller et al. (1996) also obtained an age of 2627 ± 8 Ma for weakly foliated granite northwest of Cue. Slightly older than the recrystallized monzogranites mentioned above is a tonalite from near Cue, which was dated using single zircon grain conventional U–Pb methods at 2759 ± 4 Ma (Pidgeon and Hallberg, 2000). This age is similar to ages for nearby felsic volcanic rocks, and is interpreted to reflect their coeval development (Pidgeon and Hallberg, 2000). High-HFSE granite from the Cue area has a similar SHRIMP U–Pb zircon age of c. 2745 Ma (Champion and Cassidy, 2002). Slightly younger are porphyritic granodiorite–tonalite dykes, intruded into steeply dipping foliated greenstones at the Big Bell Mine just west of Cue (Fig. 2) that have a SHRIMP U–Pb zircon age of 2737 ± 4 Ma (Mueller et al., 1996).

While there are no directly obtained data of older crustal rocks in the northern Murchison Domain there is some evidence to suggest that it developed on c. 3000 Ma crust (Pidgeon and Hallberg, 2000; Champion and Cassidy, 2002). Drillcore samples of mixed felsic, mafic, and ultramafic volcanic rocks from the southern part of the Yalgoo–Singleton greenstone belt (Fig. 3) have a Sm–Nd whole-rock isochron age of 2980 ± 0.12 Ma (Fletcher et al., 1984). Zircon populations of about that age in felsic volcanic rocks have been interpreted as being inherited from this crust (Pidgeon and Hallberg, 2000). Gneisses in the southern Murchison Domain have ages of 3007 ± 3 and 2940 ± 5 Ma, and mafic granites in the Southern Cross Domain have zircon populations of c. 3020 Ma (Deception Hill microgranite, possibly inherited grains) and 2800 Ma (Courbarloo granite, possibly related to the Kantie Murdana Volcanics; Champion and Cassidy, 2002). The common occurrence of inherited zircons in younger rocks of the northern Murchison Domain suggests that older, c. 3000 Ma granitic rocks are also present in this region (Champion and Cassidy, 2002). Neodymium-model ages of c. 3.3 to 3.1 Ga from granitic rocks of the Murchison Domain indicate that they mainly evolved from slightly older crustal sources; however, in the Meekatharra area the model ages indicate slightly younger crustal sources of c. 3.1 to 2.9 Ga (Cassidy et al., 2002).

Mafic dykes

Abundant crosscutting mafic dykes are prominent on the aeromagnetic images, have mainly easterly trends, and can be more than 200 km long. They are mostly Mesoproterozoic and part of either the 1210 Ma Marnda Moorn large igneous province (LIP) or the 1075 Ma Warakurna LIP (Wingate et al., 2004, 2005). Some may also be part of the c. 2411 Ma Widgiemooltha dyke swarm (Myers, 1990, and references therein). A few of the dykes in the interpreted map area trend northwest and are probably part of the Boyagin swarm and Marnda Moorn LIP. On aeromagnetic images the dykes have strong signatures that are either magnetic highs or lows. Some have subcircular patterns and are more likely to be sills (e.g. on KIRKALOCKA, Fig. 2).

Methodology used to create the interpreted bedrock geology map

The interpreted bedrock geology map has been compiled in a GIS environment (ArcMap) to provide maximum spatial accuracy, and to facilitate the use of a number of datasets as layers. This allows interpretations of specific features to be made by directly comparing information from each dataset at specific locations. This not only improves the interpretation of individual features themselves, but also enhances our understanding of their signatures in each dataset (e.g. aeromagnetic signature compared to particular band combinations in satellite imagery).

Datasets and data sources — purpose and limitations

The datasets used in this compilation include:

- aeromagnetic data flown at 400-m line spacing, with some 200-m line spacing data stitched in where available as open-file data;
- Landsat TM, mostly as RGB images with band combinations of 7:4:1 and 7:5:4;
- ASTER satellite imagery, including decorrelation stretches of the principal components of the 15 m bands 1, 2, and 3;
- radiometric data flown at 400-m line spacing, shown as ternary images where red = potassium, green = thorium, blue = uranium, black = none of these present, white = all of these present;
- gravity data (11 × 11 km station grid);
- GSWA 1:250 000-scale geological series map sheets;
- the 1:100 000-scale maps of J. A. Hallberg (Hallberg, 2000; and Geological Survey of Western Australia, 2006);
- 1:500 000-scale maps from Watkins and Hickman (1990a);
- map of the Windimurra Intrusion from Mathison et al. (1991);
- map and information on granitic rocks around the Jack Hills Belt, Narryer Terrane from Pidgeon and Wilde (1998);
- 2005 GSWA fieldwork.

Aeromagnetic data for the images used were reduced to pole to correct the positions of the anomalies. These were then used to create the first vertical derivative images. Because the project covered a large area, the data were also subset into smaller sections to focus on areas of interest and allow more detailed image enhancement. Structures were interpreted from the aeromagnetic images by tracing out the regional structural trendlines. Locations of faults and geological boundaries were in part interpreted by identifying truncations and discontinuities in the trendlines. First vertical derivative images were primarily used in order to trace the locations of these features as near to the surface as possible. Most of the trendlines follow magnetic highs, but include some linear

lows. It should be noted that although the map is intended as a surface solid geology map, some of the features picked up by the trendlines are subsurface, particularly where weathering conceals their magnetic signature at or near the surface. Furthermore, if they represent features that dip, then they would outcrop at a slightly different location to where the subsurface high is located on the 2D image, that is, where the dipping magnetic high would intersect the surface. Dykes were excluded from the structural layer because they are numerous and do not necessarily coincide with structural (deformational) trends. However, some intrusions, a few of which may be subsurface, were delineated. No attempt was made to determine lithological character with magnetic trendlines (commonly called worm maps), but the magnetic character of the rocks was used to help interpret the bedrock geology (see below). Some fold closures could be determined from the trendlines, although these were limited to large-scale folds because the 400-m line spacing data provides a maximum of 80 to 100 m ground resolution, and the 200-m line spacing data a maximum of 50 to 70 m. This highlights the limitations of interpreting structural geology from such datasets — for example, it is sometimes difficult to distinguish apparent closures from truncations of two intersecting anomalies. Thus, small-scale folds and structures, an important component of understanding the larger scale structural geology of a region, are not visible using this methodology. To help overcome these ambiguities and the lack of detail, the faults and folds shown on the interpreted bedrock map were based on a combination of all the datasets and new fieldwork where possible, and not just the aeromagnetic images.

Faults on the map are divided by type where known, and as major or minor faults (denoted by line thickness). Major faults are defined as having greater length and more displacement than minor faults. Where magnetic anomalies are offset, the displacement direction (dextral or sinistral) is shown — this is apparent direction only (i.e. interpreted from 2D imagery) and should not be assumed to be strike-slip offset. Faults shown as interpreted are commonly under cover, but this is not always the case because the aeromagnetic images can sometimes show faults that are not obvious through outcrop. Many of the faults on the map are associated with magnetic lows, and these commonly coincide with major quartz veins. Some major strike-slip shear zones (e.g. the Chunderloo Shear Zone) are delineated by strong trendlines with sigmoidal splays that also indicate shear sense.

Fault dip is difficult to estimate based on the aeromagnetic images, particularly as many of the greenstone belts contain highly magnetic BIF and ultramafic rocks that show remanence effects. Thus interpretation of dip is difficult because the magnetic gradients may be unrealistic. Published maps available for the map area contain almost no information on fault dip or relative movement. These features, where shown on the structural layer, have been constrained by structural fieldwork undertaken in 2005, and are largely confined to the northern half of the project area. Structures in the Jack Hills Belt in the northwestern part of the project area are based on mapping by C. V. Spaggiari in 2003 and 2004 at Curtin University, Perth (Spaggiari, in prep.).

Surface datasets such as Landsat, ASTER, and radiometrics provide a means to interpret lithological contacts and, in conjunction with the geological maps, to determine lithologies. Because the surface datasets are georeferenced, they also allow lithological contacts to be drawn more accurately spatially than the geological maps because that mapping was done before the availability of orthophotography and, in the case of the GSWA 1:250 000-scale maps, before the availability of GPS information. In some parts of the interpreted bedrock geology map, lithological trendlines have been drawn from the satellite images to highlight lithological variation not shown by the aeromagnetic trends. These sometimes delineate fold closures not visible on the aeromagnetic images, for example, the Mount Mulcahy synform just south of the Weld Range greenstone belt (Fig. 2).

The compilation of the bedrock geology layer and, to a lesser extent, the structural geology layer was greatly facilitated by the published GSWA 1:250 000-scale geological series maps (Belele, Cue, Kirkalocka, Ninghan, Glengarry, Sandstone, Youanmi, Barlee, see Fig. 2 for locations) and, where coverage was available, by the 1:100 000-scale maps of J. A. Hallberg (Hallberg, 2000). The latter in particular proved very useful and have been incorporated into the bedrock geology layer. This required simplifying and grouping the units for the scale of map presented here, and the original maps should be used where more detailed lithological information is required. Limited fieldwork undertaken in 2005 concentrated on structural mapping, and so most of the bedrock interpretation is based on previous mapping. The aeromagnetic images do not provide a direct indication of lithologies, but may be used very effectively to extrapolate information from both field mapping and satellite imagery under cover. The bedrock geology layer includes mafic dykes interpreted from the aeromagnetic images, and drawn from published maps. It follows that some of the dykes interpreted from the aeromagnetic images are under cover and may also be subsurface, that is, not just covered by regolith.

Interpreted regional geology

Interpretation of the new aeromagnetic images, combined with other datasets and fieldwork, has allowed preliminary revision of the published maps and structural schemes. This will be updated as more detailed 1:100 000-scale mapping is carried out by GSWA in the Murchison Domain. From the interpretation presented here, it is apparent that the dominant regional structures are northeast-trending and north- to northwest-trending folds, faults, and shear zones. Early east-trending folds (D_2 of Watkins and Hickman, 1990a) are preserved locally, but may be confined to the west of a major west-dipping thrust, here named the Carbar Fault, that separates the Weld Range and Mingah Range greenstone belts from the Meekatharra–Wydgee greenstone belt (Fig. 2). Near Cue the Carbar Fault broadly coincides with the Big Bell Fault of Watkins and Hickman (1990a), as does the southwestern part of the Chunderloo Shear Zone (Figs 2 and 3). Pidgeon and Hallberg (2000) also showed a fault extending north

of the Big Bell Fault as far as the Weld Range greenstone belt, but did not indicate the type of fault or show its extension to the north (Fig. 5). Myers and Hocking (1998) showed an arcuate, west-dipping thrust that cut across the northern part of the Dalgaranga greenstone belt, extended northeast to coincide with the Big Bell Fault near Cue, then east of the Weld Range greenstone belt, near Barloweerie Peaks. Rocks on either side of the Carbar Fault appear to have different structural styles and may represent two distinct structural domains.

One of the main differences between the map presented here and previous work is the identification of the Meekatharra structural zone (Fig. 2) east of the Carbar Fault, and west of the Mount Magnet Fault and Polelle synform. This is a major, northeast-trending shear-dominated zone, about 50 to 60 km wide, incorporating the Meekatharra area and extending through the Cue region as far south as Mount Magnet (taking in a large part of the Meekatharra–Wydgee greenstone belt). At Mount Magnet the structural zone changes to a northerly trend where faults and shears cut through granitic rocks and the Windimurra and Narndee Intrusions. In the aeromagnetic images southwest of the Windimurra Intrusion, and within the inferred continuation of the Meekatharra structural zone, tight north-trending folds are evident within interpreted granitic rocks under cover. Fieldwork in 2005 was confined to the northern half of the map area so most of the following detailed descriptions and interpretations relate to that region.

Eastern region — Meekatharra structural zone

The northeast-trending Meekatharra structural zone is dominated by north- and northeast-trending folds and shears, including refolded folds with approximately co-planar fold axes (Geological Survey of Western Australia, in prep.b). Many of the folds are truncated by shears or faults, and the structural zone is interpreted as a major zone of shear-related deformation. The most prominent shear zone is the northeast-trending Chunderloo Shear Zone that shows up clearly on the aeromagnetic images and has a sigmoidal pattern indicative of dextral kinematics (Fig. 2). The shear zone is predominantly within granitic rocks, which typically show dextral kinematic indicators such as feldspar porphyroclasts and S–C foliations (Fig. 6a,b). Similarly oriented dextral shear zones can be seen on the aeromagnetic images in the southern and central parts of the map, including the likely southern continuation of the Meekatharra structural zone, one of which cuts across the northwestern margin of the Narndee Intrusion (Fig. 2). The Meekatharra structural zone broadly coincides with a zone of granitic rocks whose Nd-model ages indicate that they evolved from slightly younger crust (c. 3.1 to 2.9 Ga) than the surrounding granites (c. 3.3 to 3.1 Ga; Cassidy et al., 2002).

In the footwall region of the Carbar Fault, east of the Weld Range greenstone belt and west of the Chunderloo Shear Zone (Fig. 2), most rocks have a steep west-dipping, strong foliation, and moderate northwest- or southwest-plunging mineral lineation (see also Elias, 1982 and Watkins et al., 1987). Within the greenstones the mineral lineation is locally parallel to fold axes of tight to isoclinal folds that fold an earlier foliation, and the regional foliation is axial planar to these folds. These folds are overprinted by small shears, brittle faults, and a localized, mostly northwest trending, spaced crenulation cleavage.

East of the Weld Range greenstone belt and Barloweerie Peaks (Fig. 2), granitic rocks are locally banded and have a strong, penetrative, northeast-trending and west-dipping foliation that is mylonitic in places (Fig. 7a). These granites are folded into a kilometre-scale, northeast-plunging antiform, along with the greenstones of Barloweerie Peaks (primarily metadolerite). The fold has a synformal parasitic fold on its eastern limb, and is probably a second-generation fold as a foliation in the greenstones is folded (Fig. 7b). Small-scale folds of both metadolerite and granite and pegmatite are preserved in the core of the fold, and its axial-planar foliation dips steeply to the west-northwest, parallel to the regional foliation (Fig. 7c). The fold is probably truncated on the eastern side by a west-dipping fault or shear (Fig. 2), which is indicated by the presence of strongly deformed and mylonitic granites (Figs 2, 7a). North of Barloweerie Peaks the fold closure appears to pinch out within the greenstones, and is possibly truncated by another shear to the west. Another similar antiformal fold is interpreted

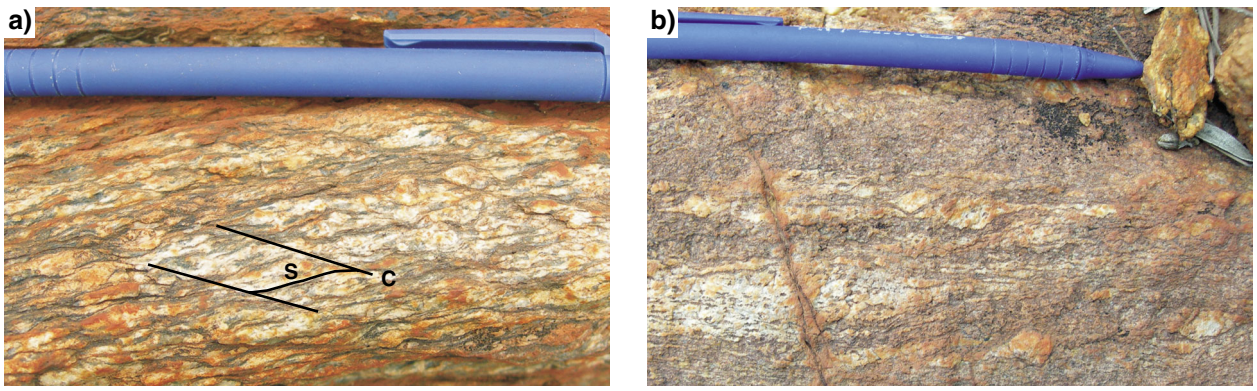

CS8 09.05.06

Figure 6. Dextral kinematic indicators in the Chunderloo Shear Zone: a) S–C foliations in granite (MGA 629755E 7041230N); b) K-feldspar porphyroclasts showing dextral asymmetry (MGA 633078E 7044439N)

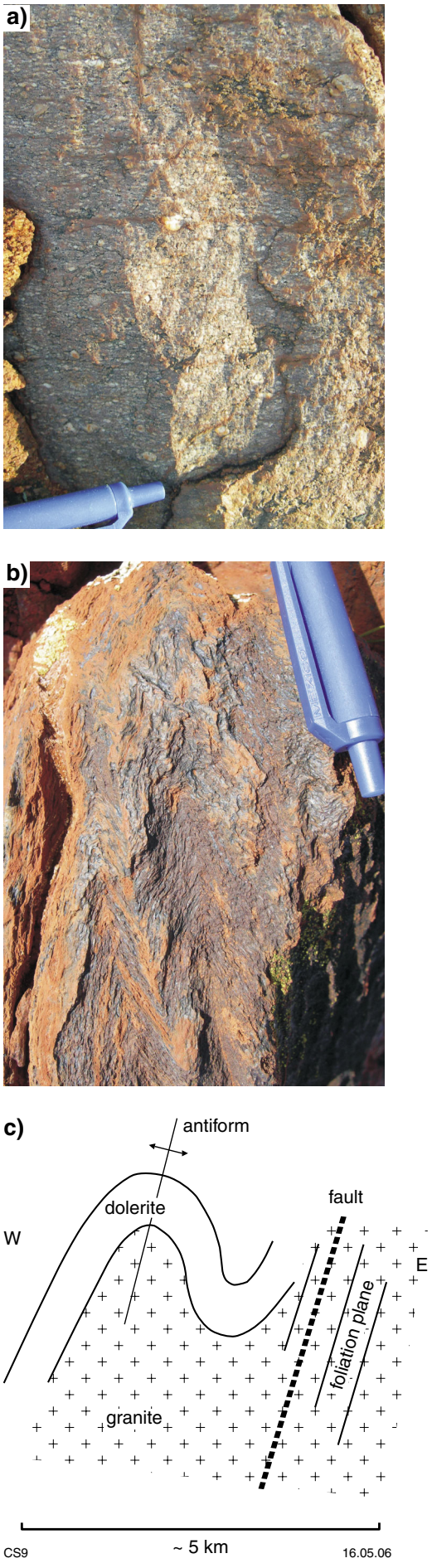

in the aeromagnetic data under cover just to the east and is probably in granitic rocks (Fig. 2). This fold is either truncated by, or formed coevally with, the Chunderloo Shear Zone.

Western region — Weld Range and Mingah Range greenstone belts

The region to the west of the Carbar Fault is less well understood than the Meekatharra structural zone to the east. The deformation is variable with complex geometric patterns, and is less shear dominated. Evidence of possibly early, east-trending structures are preserved at Mount Mulcahy (Fig. 2), south of the east-northeasterly trending Weld Range greenstone belt, and as isoclinal folds within BIF on the southern side of the Weld Range greenstone belt. However, in the northwestern part of the Mingah Range greenstone belt, quartzites that are folded into a tight to isoclinal, potentially overturned syncline (Elias, 1982) contain detrital zircons with ages as young as c. 2650 Ma (Geological Survey of Western Australia, in prep.c), indicating that the east-trending folding there is relatively young. Much of the western side of the Carbar Fault, including the east-trending fold at Mount Mulcahy, shows evidence of an overprinting northeast-trending foliation, possibly related to formation of the thrust. These relationships show that the thrust clearly post-dates the majority of granitic rocks and may be a relatively late structure.

The Carbar Fault is exposed at the northeastern end of the Weld Range greenstone belt where BIF and dolerite of the belt are topographically higher than granitic rocks to the east. A thrust relationship is indicated by a sharp contact and asymmetric, east-verging folds with subhorizontal plunges in BIF in the hangingwall (Fig. 8a,c). Small, asymmetric, moderately southwest plunging kink folds in BIF, oblique to the fault contact, and sinistral shear bands indicate a possible sinistral strike-slip component to the thrust movement. These features, and the subhorizontally plunging folds, fold both bedding and a foliation, and appear to be of the same generation. Numerous, approximately northeast- and northwest-trending (strike perpendicular) conjugate kink folds and brittle faults throughout the Weld Range greenstone belt are also probably related to formation of the thrust. Along the southern margin of the BIF section of the belt, these structures overprint tight to isoclinal folds that are subparallel to bedding in the BIF (Fig. 8b). These folds may relate to a faulted contact between BIF and dolerite of the Weld Range greenstone belt and felsic volcanic rocks and basalt to the south (Fig. 2). They typically have Z-asymmetry that suggests an antiform to the north, but

Figure 7. Structural relationships at Barloweerie Peaks: a) mylonitic granite from fault zone east of the antiform (MGA 600477E 7034343N); b) tight folds in second-generation antiformal fold core showing folded foliation in dolerite (MGA 599092E 7040329N); c) schematic section of interpreted structures

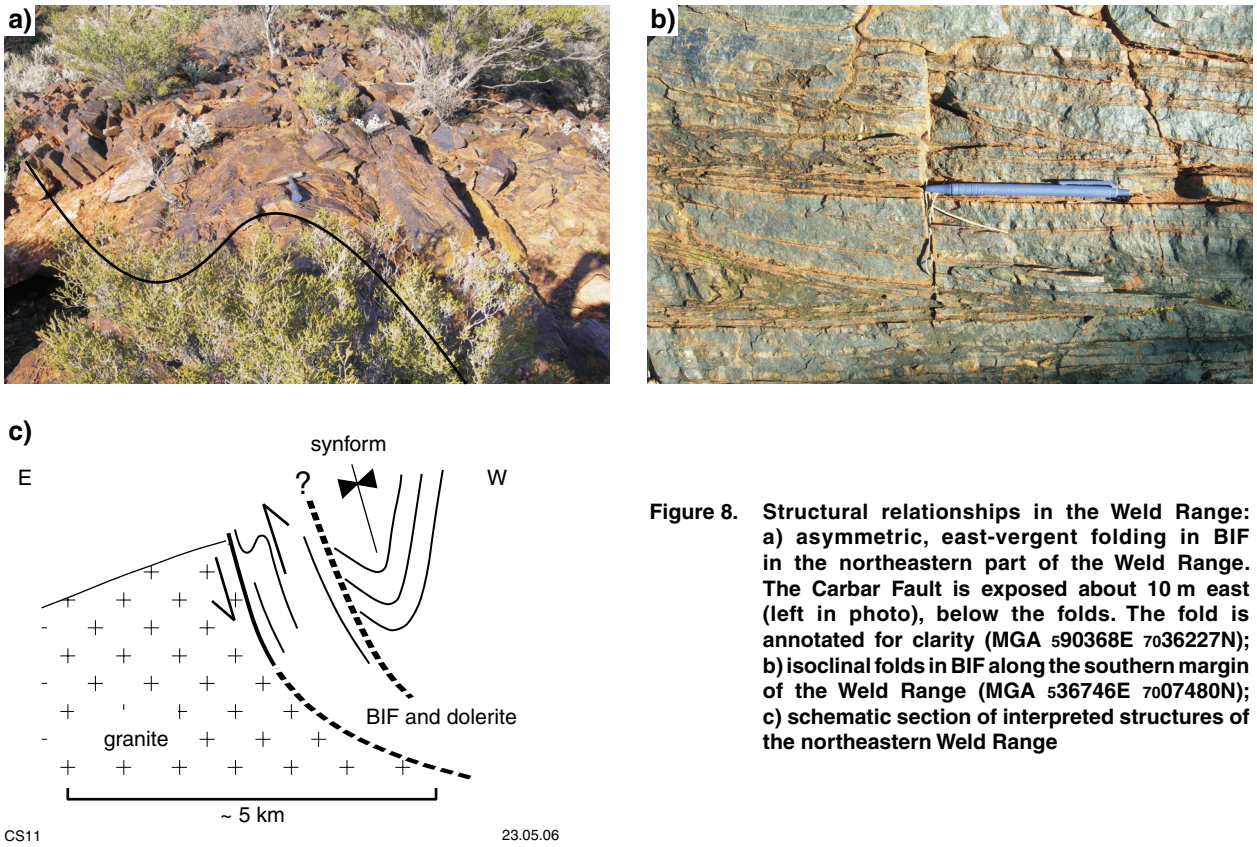

Figure 8. Structural relationships in the Weld Range: a) asymmetric, east-vergent folding in BIF in the northeastern part of the Weld Range. The Carbar Fault is exposed about 10 m east (left in photo), below the folds. The fold is annotated for clarity (MGA 590368E 7036227N); b) isoclinal folds in BIF along the southern margin of the Weld Range (MGA 536746E 7007480N); c) schematic section of interpreted structures of the northeastern Weld Range

this changes to S-asymmetry at the southwestern end of the range and, consistent with a change in the predominant bedding dip, is indicative of a truncated tight synform along this southern margin (Fig. 2). The northern margin of the Weld Range greenstone belt shows a gradational transition from dominantly BIF to felsic volcanic rocks and associated sedimentary rocks. This is marked by a number of approximately 10 to 20 cm-thick sandstone and possible volcanic sandstone horizons within the BIF, grading to thicker lithic sandstone beds that are still within BIF but close to its margin (Fig. 9). In contrast to the southern margin, these rocks show little evidence of deformation, apart from steep bedding dips, and primary relationships are well preserved. The western end of the Weld Range greenstone belt terminates abruptly against granitic rocks. Greenstones just to the north have a northeast trend, indicating the possibility of another major northeast-trending fault (Fig. 2).

Figure 9. Lithic volcanic sandstone interbedded with BIF close to the contact with felsic volcanic rocks and the northern margin of the Weld Range

The relationship between the Mingah Range greenstone belt and the Weld Range greenstone belt is unclear. The belts are perpendicular to each other, separated by a large monzogranite mass that contains xenoliths or attenuated slivers of greenstone (Fig. 2). One of these extends about 20 km off the northeastern tip of the Weld Range greenstone belt and trends northwest, parallel to the Mingah greenstone belt, and another extends about 17 km from the western side of the Mingah greenstone belt and trends parallel to the Weld Range greenstone belt. It is possible that these belts were related before intrusion of the granite. However, they differ lithologically in that the Weld Range greenstone belt is dominated by BIF and dolerite, whereas the Mingah Range greenstone belt contains a greater range of rock types including metabasalts, differentiated sills of gabbro, pyroxenite, and ultramafics, with only minor local BIF on the western margin (see also Elias, 1982). Both greenstone belts contain felsic volcanic rocks and associated sedimentary rocks.

The northwest trend of the Mingah Range greenstone belt is unlike that of any other belt in the region. Most

rocks in the belt have a northwest-trending, steeply northeast or southwest dipping foliation of variable strength that is axial planar to both (locally) small-scale F_1 and F_2 tight folds. The F_2 folds also fold a strong lineation in the metabasaltic rocks that is parallel to moderately to steeply, predominantly southerly plunging fold axes of F_1 folds. These folds and foliations are overprinted by a northeast- or north-trending foliation and associated tight folds, which are particularly evident in the southeast, adjacent to the Carbar Fault. This suggests that the deformation that produced the regional trend of the Meekatharra structural zone post-dates the northwest-trending structures in the Mingah Range greenstone belt, as does the truncation of both the Weld Range and Mingah Range greenstone belts by the Carbar Fault. One possible explanation for the unusual trend of the structures in the Mingah Range greenstone belt, and of the belt itself, is rotation and disruption or displacement of the greenstones during granite emplacement. However, the timing of the deformation events relative to granite emplacement is not clear. Although parallel to the trend of the Mingah Range greenstone belt, late northwest-trending brittle faults that cut through the Weld Range greenstone belt have only small displacements in the order of 1 km or so, and are not interpreted to have affected the geometry of the belt in a major way.

South of the Weld Range greenstone belt, northwest of Coodardy (on CUE, Fig. 2), strongly deformed mafic (amphibolite) xenoliths show evidence of refolding within the host granite. Isoclinally folded veins and a strong foliation within the xenoliths are refolded into upright, tight, moderately south plunging folds that have a low-grade, spaced axial-planar foliation subparallel to the northeast-trending regional foliation (Fig. 10). This suggests that the northeast-trending folding post-dates the granites, and that the earlier, higher grade folded foliation and isoclinal folds in the xenoliths may have formed during, or prior to, intrusion because the granite only shows evidence of the lower grade, weaker foliation, and no effects of particularly high strain.

Age of deformation

There is very little control on the age of the main deformation events throughout the Murchison Domain, but most granitic rocks show at least some effects of deformation, much of which may have been strongly partitioned within the granite–greenstone sequences. Given the relationships described above, it is likely that at least the main northeast-trending deformation in the Meekatharra structural zone was either synchronous with

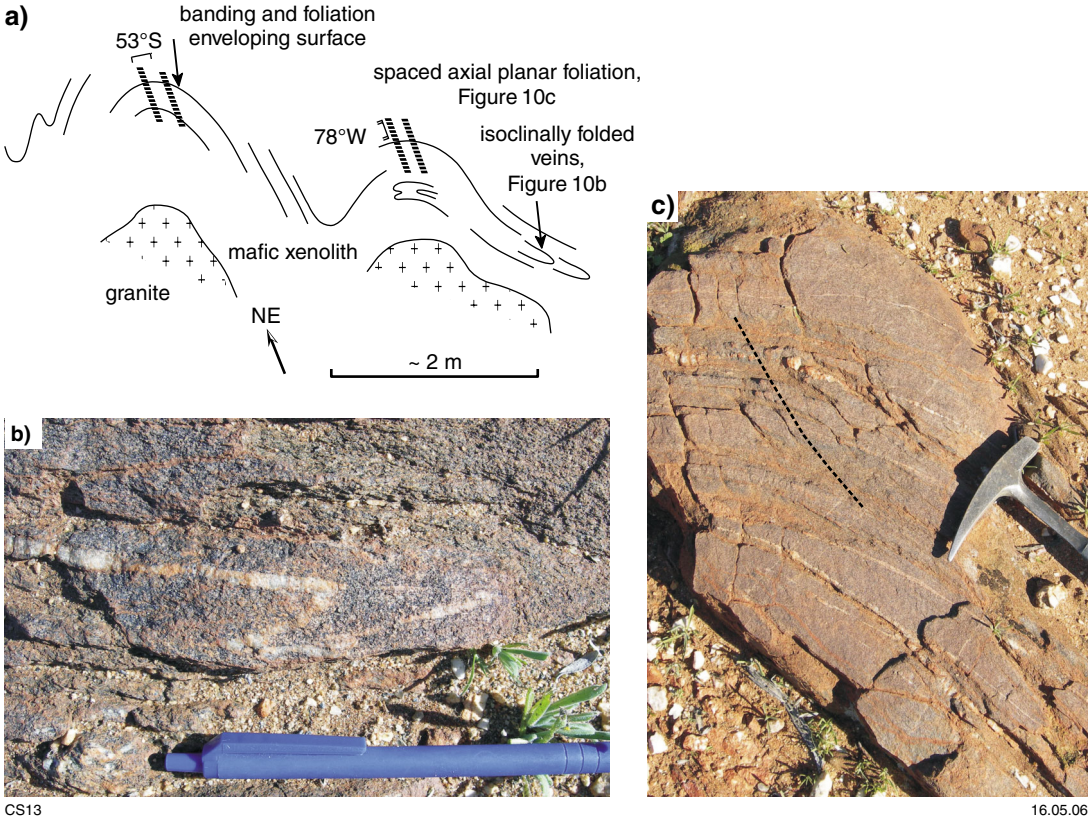

Figure 10. Granite and xenolith field relationships near Coodardy: a) sketch outcrop map of folded mafic xenolith in granite. Isoclinally folded quartz veins and a strong foliation are refolded into upright, northeast-trending folds interpreted to post-date granite intrusion; b) photo of isoclinal folds, see (a) for location; c) Photo of second generation fold, see a) for location. The dashed line marks the spaced axial-planar foliation

or post-dates most of the granites, that is, it is c. 2650 Ma or younger. Northeast-trending folds in at least some granitic rocks (e.g. at Barloweerie Peaks) suggest that the latter is more likely. An earlier deformation in the Meekatharra structural zone is indicated by refolded folds and an earlier foliation in places. The presence of complex shear-related deformation such as that seen in the Meekatharra structural zone makes simple regional structural schemes (e.g. D_1, D_2, and so on, of Watkins and Hickman, 1990a) problematic. The timing of deformation is even less clear west of the Meekatharra structural zone, although it is evident that some of the structures there are overprinted by those formed in one or both of the Meekatharra structural zone or the Carbar Fault.

Paleoproterozoic reactivation

Part of the structural complexity in the region also arises from the possibility of coplanar or coaxial reactivation or reworking of older structures, such as potential early easterly trending folds being overprinted by much younger east-trending structures, as well as by Mesoproterozoic dykes. Just north of the northwestern end of the Mingah Range greenstone belt, steeply northerly dipping, east-northeasterly trending faults and shears cut through granitic rocks (Fig. 2). These are locally mylonitic and have moderately to steeply northeasterly plunging mineral lineations that include white mica. In places dextral S–C foliations suggest oblique normal displacement, with the north side down. The shears are subparallel to large quartz veins, probably associated with the approximately east-northeasterly trending faulting in this area that links in with larger scale, approximately easterly trending faults and shears visible on the aeromagnetic images. The faults also cut through and truncate the northwestern end of the Mingah Range greenstones, and may form part of the boundary between the Narryer Terrane and Youanmi Terrane (Yalgar Fault of Myers and Hocking, 1998). Just north of this, a major east-trending dextral transpressional shear zone cuts through the Jack Hills greenstone belt (Fig. 2; Spaggiari and Hollingsworth, 2003; Spaggiari et al., 2004; Spaggiari, in prep.). Structural analysis and Ar–Ar ages from white micas from sheared rocks in the Jack Hills greenstone belt suggest that this structure formed during the Paleoproterozoic Capricorn Orogeny, but it may also be a reactivated older structure, perhaps related to formation of the Narryer Terrane and Youanmi Terrane boundary (Spaggiari et al., 2004; Spaggiari, 2005; Spaggiari in prep.). It is unclear if these east-trending faults truncate the northeast-trending Meekatharra structural zone, but aeromagnetic images suggest this may be the case. The faulting may also be related to late, east-trending open folds and warps present in the Meekatharra area (Hallberg, 2000; Geological Survey of Western Australia, in prep.b).

Mineralization controls

Gold mineralization within the Murchison Domain is concentrated within greenstone belts and is structurally controlled (e.g. Watkins and Hickman, 1990a). Historic gold deposits (from the Department of Industry and Resources' mines and mineral deposits information, MINEDEX, database) appear to be particularly abundant and focused within the Meekatharra structural zone (Fig. 11), highlighting the importance of understanding the detailed structural evolution of this zone. It is not known whether the Meekatharra structural zone is purely a structural feature superimposed on a pre-existing, laterally extensive granite–greenstone terrane, or whether it was fundamentally different to other parts of the domain from an early stage. The latter possibility is suggested by the slightly younger Nd crustal source model ages in this area (Cassidy et al., 2002) and apparent difference in style of early structures compared to the region west of the Carbar Fault. More detailed work on stratigraphic relationships of the various greenstone belts may help to resolve this issue.

Summary of outstanding issues

The brief review of the stratigraphy and structure of the Murchison Domain presented here has identified a number of aspects of the geology that require more detailed investigation. Several major faults and shears have been identified in the aeromagnetic images. However, their geometry, relative timing, and movement history (kinematics) are largely undocumented, apart from some areas in the north where there has been limited new fieldwork. These structures are integral to an understanding of how the different components of the Murchison Domain, particularly the different greenstone belts, were juxtaposed. An understanding of the relationships between greenstone belts is necessary in order to understand stratigraphic relationships and controls on mineralization. The relationship of the folding to these major structures and how it fits with regional structural schemes is also problematic, particularly in terms of addressing whether the fold superposition model of Watkins and Hickman (1990a) is relevant to the whole domain.

One of the main features identified in the interpreted bedrock geology map is the Meekatharra structural zone, which takes in a large part of the Meekatharra–Wydgee greenstone belt. In the Meekatharra area it includes at least one major shear zone. However, the structural character of this zone is not well understood around and south of Cue. The western side of the Meekatharra structural zone is marked by a major west-dipping thrust (the Carbar Fault), but the nature of the eastern side is less well known. The change in trend of the structural zone near Mount Magnet is also problematic, but may be related to the spatial distribution of granitic rocks.

Whether the Carbar Fault continues southwest is not clear from the aeromagnetic images (Fig. 2). It may link into an interpreted fault on the eastern side of the Mount Charles area of the Dalgaranga greenstone belt (Fig. 2) or cut through granitic rocks to the south (or both). Major shears flank both the eastern and western sides of the Windimurra Intrusion. On the aeromagnetic images they appear to have strike lengths of up to 90 km or so, but their

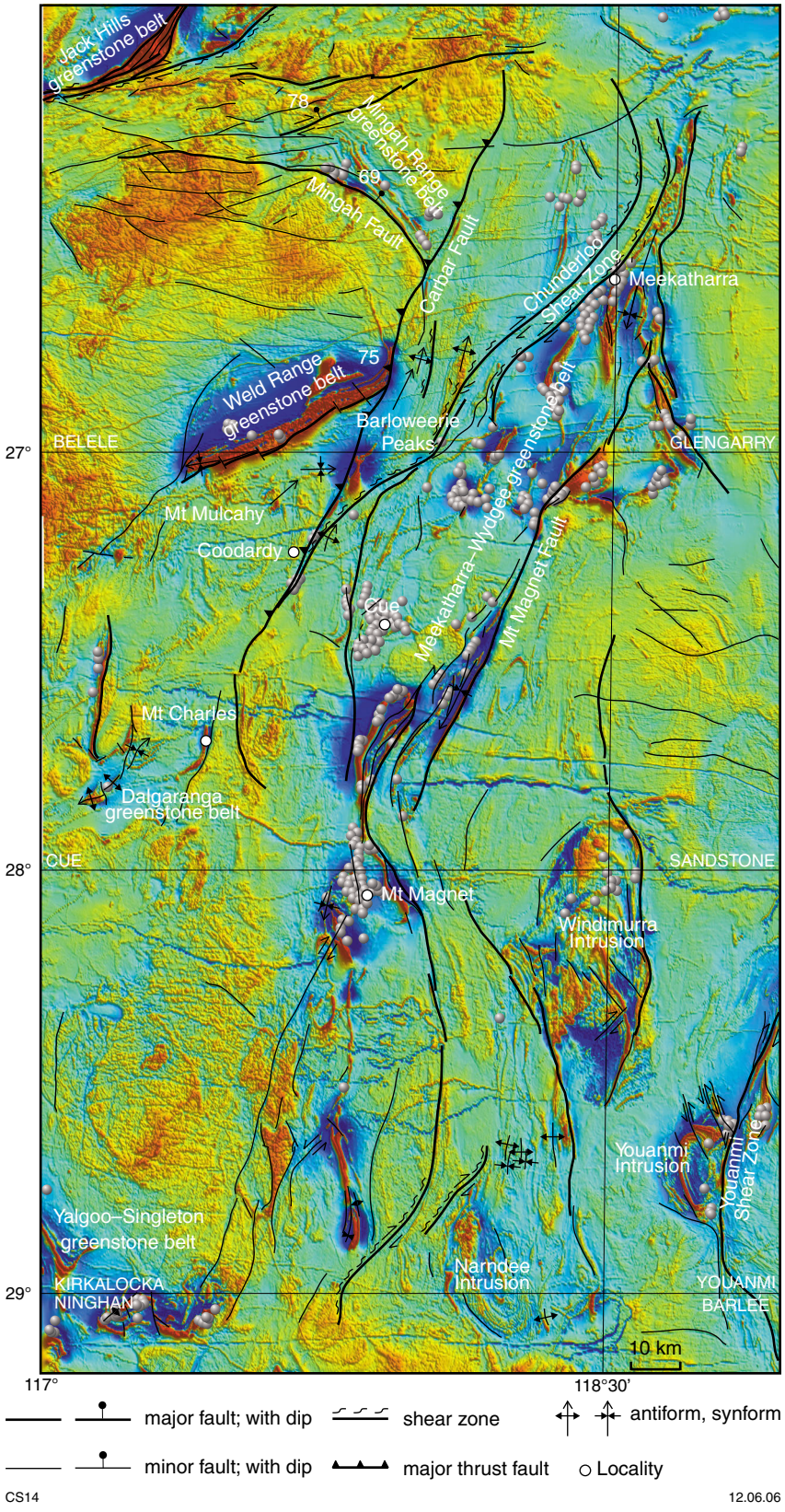

Figure 11. Simplified interpreted structural map of the northern Murchison Domain showing historic (MINEDEX database) gold deposits (grey balls). Structures shown are derived from the interpreted bedrock geology map in Geological Survey of Western Australia (2006), Hallberg (2000), GSWA's 1:250 000-scale geological series maps, and Watkins and Hickman's (1990a) 1:500 000 geological map

geometry and kinematics are not known. The shear on the western side of the Windimurra Intrusion is adjacent to strongly deformed granitic rocks that may link to the continuation of the Meekatharra structural zone, south of Mount Magnet.

Both the relative and absolute timing of major deformation events in the Murchison Domain are unknown. Recent geochronology has shown that previous interpretations of 'post-folding' and 'post-tectonic' granites are unreliable and cannot be used to determine structural chronology. Although difficult to locate, only intrusions that clearly crosscut deformation-related structures should be selected for dating. Unfoliated granites may simply show the effects of strain partitioning.

References

AHMAT, A. L., and RUDDOCK, I., 1990, Windimurra and Narndee layered complexes, *in* Geology and mineral resources of Western Australia: Western Australia Geological Survey, Memoir 3, p. 119–126.

CHAMPION, D. C., and CASSIDY, K. F., 2002, Granites of the northern Murchison Province: their distribution, age, geochemistry, petrogenesis, relationship with mineralisation, and implications for tectonic environment, *in* Characterisation and metallogenic significance of Archaean granitoids of the Yilgarn Craton, Western Australia: Perth, Western Australia, Minerals and Energy Research Institute of Western Australia, Report no. 222, p. 60.

CASSIDY, K. F., CHAMPION, D. C., KRAP Z, B., BARLEY, M. E., BROWN, S. J. A., BLEWETT, R. S., GROENEWALD, P. B., and TYLER, I. M., 2006, A revised geological framework for the Yilgarn Craton, Western Australia: Western Australia Geological Survey, Record 2006/8, 8p.

CASSIDY, K. F., CHAMPION, D. C., McNAUGHTON, N. J., FLETCHER, I. R., WHITAKER, A., BASTRAKOVA, I., and BUDD, A. R., 2002, Characterisation and metallogenic significance of Archaean granitoids of the Yilgarn Craton, Western Australia: Perth, Western Australia, Minerals and Energy Research Institute of Western Australia, Report no. 222, 538p.

ELIAS, M., 1982, Belele, W.A. (1st edition): Western Australia Geological Survey, 1:250 000 Geological Series Explanatory Notes, 22p.

FLETCHER, I. R., ROSMAN, K. J. R., WILLIAMS, I. R., HICKMAN, A. H., and BAXTER, J. L., 1984, Sm–Nd geochronology of greenstone belts in the Yilgarn Block, Western Australia: Precambrian Research, v. 26, p. 333–361.

GEE, R. D., 1979, Structure and tectonic style of the Western Australian Shield: Tectonophysics, v. 58, p. 327–369.

GEOLOGICAL SURVEY OF WESTERN AUSTRALIA, 2006, Murchison geological exploration package, February 2006 update: Western Australia Geological Survey, Record 2006/2.

GEOLOGICAL SURVEY OF WESTERN AUSTRALIA, in prep.a, Central Yilgarn 1:100 000 Geological Information Series: Western Australia Geological Survey.

GEOLOGICAL SURVEY OF WESTERN AUSTRALIA, in prep.b, Murchison 1:100 000 Geological Information Series: Western Australia Geological Survey.

GEOLOGICAL SURVEY OF WESTERN AUSTRALIA, in prep.c, Compilation of geochronology data: Western Australia Geological Survey.

HALLBERG, J. A., 2000, Notes to accompany the Hallberg Murchison 1:25 000 geology dataset 1989–94: Western Australia Geological Survey, Record 2000/20 (now incorporated into GSWA, 2006, above).

MATHISON, C. I., PERRING, R. J., VOGT, J. H., PARKS, J., HILL, R. E. T., and AHMAT, A. L., 1991, The Windimurra Complex, *in* Mafic–ultramafic complexes of Western Australia *edited by* S. J. BARNES and R. E. T. HILL: Geological Society of Australia, W.A. Division, Perth, Sixth International Platinum Symposium, 1991, Excursion Guidebook No. 3, p. 45–76.

MUELLER, A. G., CAMPBELL, I. H., SCHIØTTE, L., SEVIGNY, J. H., and LAYER, P. W., 1996, Constraints on the age of granitoid emplacement, metamorphism, gold mineralization, and subsequent cooling of the Archean Greenstone Terrane at Big Bell, Western Australia: Economic Geology, v. 91, p. 896–915.

MYERS, J. S., 1990, Mafic dyke swarms, *in* Geology and mineral resources of Western Australia: Western Australia Geological Survey, Memoir 3, p. 126–127.

MYERS, J. S., and WATKINS, K. P., 1985, Origin of granite–greenstone patterns, Yilgarn Block, Western Australia: Geology, v. 13, p. 778–780.

MYERS, J. S., and HOCKING, R. M., 1998, Geological map of Western Australia, 1:2 500 000 scale (13th edition): Western Australia Geological Survey.

NELSON, D. R., 2000, 169003: vesicular rhyolite, Cannon Hill, *in* Compilation of geochronology data, October 1994 update: Western Australia Geological Survey.

PIDGEON, R. T., and HALLBERG, J. A., 2000, Age relationships in supracrustal sequences of the northern part of the Murchison Terrane, Archaean Yilgarn Craton, Western Australia: a combined field and zircon U–Pb study: Australian Journal of Earth Sciences, v. 47, p. 153–165.

PIDGEON, R. T., and WILDE, S. A., 1990, The distribution of 3.0 Ga and 2.7 Ga volcanic episodes in the Yilgarn Craton of Western Australia: Precambrian Research, v. 48, p. 309–325.

PIDGEON, R. T., and WILDE, S. A., 1998, The interpretation of complex zircon U–Pb systems in Archaean granitoids and gneisses from the Jack Hills, Narryer Gneiss Terrane, Western Australia: Precambrian Research, v. 91, p. 309–332.

PIDGEON, R. T., FURFARO, D., and CLIFFORD, B. A., 1994, Investigation of the age and rate of deposition of part of the Gossan Hill Group, Golden Grove using conventional single grain zircon U–Pb geochronology: Geological Society of Australia, Abstracts, no. 37, p. 346.

PIRAJNO, F., JONES, J. A., HOCKING, R. M., and HALILOVIC, J., 2004, Geology and tectonic evolution of Palaeoproterozoic basins of the eastern Capricorn Orogen, Western Australia: Precambrian Research, v. 128, p. 315–342.

REY, P., COSTA, S., VANDERHEAGUE, O., and FOLEY, B., 1999, Archean regional strain field in the Yilgarn Craton (WA): fold superposition or incremental strain field interferences?, *in* Last Conference of the Millenium *edited by* M. JESSELL: Geological Society of Australia, Abstracts, no. 53, p. 221.

SCHIØTTE, L., and CAMPBELL, I. H., 1996, Chronology of the Mount Magnet granite–greenstone terrain, Yilgarn Craton, Western Australia: implications for field based predictions of the relative timing of granitoid emplacement: Precambrian Research, v. 78, p. 237–260.

SPAGGIARI, C. V., 2005, Proterozoic deformation of the northwestern Yilgarn Craton, Western Australia, *in* Supercontinents and Earth Evolution Symposium *edited by* M. T. D. WINGATE and S. A. PISAREVSKY: Geological Society of Australia, Abstracts, no. 81, p. 28.

SPAGGIARI, C. V., in prep., Structural and lithological evolution of the Jack Hills greenstone belt, Narryer Terrane, Yilgarn Craton: Western Australia Geological Survey, Record.

SPAGGIARI, C. V., and HOLLINGSWORTH, D., 2003, Structural analysis and tectonic setting of the Jack Hills Belt, northern Yilgarn margin, Western Australia: Geological Society of Australia, Abstracts, no. 72, p. 52.

SPAGGIARI, C. V., PIDGEON, R. T., and WILDE, S. A., 2004, Structural and tectonic framework of >4.0 Ga detrital zircons from the Jack Hills Belt, Narryer Terrane, Western Australia: Geological Society of America, Abstracts, v. 36(5), p. 207.

WANG, Q., SCHIØTTE, L., and CAMPBELL, I. H., 1998, Geochronology of supracrustal rocks from the Golden Grove area, Murchison Province, Yilgarn Craton, Western Australia: Australian Journal of Earth Sciences, v. 45, p. 571–577.

WATKINS, K. P., and HICKMAN, A. H., 1990a, Geological evolution and mineralization of the Murchison Province, Western Australia: Western Australia Geological Survey, Bulletin 137, 267p.

WATKINS, K. P., and HICKMAN, A. H., 1990b, Excursion No. 2: Murchison granite–greenstone terrain, *in* Third International Archaean symposium, excursion guidebook *edited by* S. E. HO, J. E. GLOVER, J. S. MYERS, and J. R. MUHLING: The University of Western Australia, Geology Key Centre and University Extension, Publication No. 21, p. 145–201.

WATKINS, K. P., TYLER, I. M., and HICKMAN, A. H., 1987, Cue, W.A. (2nd edition): Western Australia Geological Survey, 1:250 000 Geological Series Explanatory Notes, 31p.

WEIDENBECK, M., and WATKINS, K. P., 1993, A time scale for granitoid emplacement in the Archaean Murchison Province, Western Australia, by single zircon geochronology: Precambrian Research, v. 61, p. 1–26.

WINGATE, M. T. D., PIRAJNO, F., and MORRIS, P. A., 2004, Warakurna large igneous province: A new Mesoproterozoic large igneous province in west-central Australia: Geology, v. 32, p. 105–108.

WINGATE, M. T. D., MORRIS, P. A., PIRAJNO, F., and PIDGEON, R. T., 2005, Two large igneous provinces in Late Mesoproterozoic Australia, *in* Supercontinents and Earth Evolution Symposium *edited by* M. T. D. WINGATE and S. A. PISAREVSKY: Geological Society of Australia, Abstracts, no. 81, p. 151.

YEATS, C. J., McNAUGHTON, N. J., and GROVES, D. I., 1996, SHRIMP U–Pb geochronological constraints on Archean volcanic-hosted massive sulfide and lode gold mineralization at Mount Gibson, Yilgarn Craton, Western Australia: Economic Geology, v. 91, p. 135–1371.

SPAGGIARI

Interpreted bedrock geology of the northern Murchison Domain, Youanmi Terrane, Yilgarn Craton

RECORD 2006/10

This Record is published in digital format (PDF) and is available online at: www.doir.wa.gov.au/gswa/onlinepublications. Laser-printed copies can be ordered from the Information Centre for the cost of printing and binding.

Further details of geological publications and maps produced by the Geological Survey of Western Australia can be obtained by contacting:

Information Centre
Department of Industry and Resources
100 Plain Street
East Perth WA 6004
Phone: (08) 9222 3459 Fax: (08) 9222 3444

www.doir.wa.gov.au/gswa/onlinepublications